

The crystal structure of schairerite and its relationship to sulphohalite

L. FANFANI, A. NUNZI, P. F. ZANAZZI, A. R. ZANZARI

Istituto di Mineralogia, Università di Perugia, Perugia, Italy

AND C. SABELLI

Istituto di Mineralogia, Università di Firenze, Firenze, Italy

SUMMARY. The crystal structure of schairerite from Searles Lake, California, has been determined employing X-ray diffraction data collected on a single-crystal diffractometer. The crystal structure was refined by least-squares methods employing isotropic thermal parameters to a final *R* index of 0.07 for 2536 independent observed reflections. The cell content is $3[\text{Na}_{21}(\text{SO}_4)_7\text{F}_6\text{Cl}]$. The space group is *P31m* with *a* 12.197 Å and *c* 19.259 Å. Schairerite exhibits a marked sub-cell (*a* 7.042 Å, the same *c* axis and *P3m1* symmetry), which may be related to the unit cell of sulphohalite when described in a hexagonal lattice.

The crystal structure of schairerite may be considered as consisting of seven sheets of Na^+ ions perpendicular to the *c* axis. These sheets are connected to each other, building up a three-dimensional framework. The Na^+ ions in these sheets are arranged in an array built up of hexagons and triangles. Sulphur atoms lie in the sheets at the centres of each hexagon, the halogen atoms lying between the sheets midway between the centres of two triangles. A comparison with sulphohalite shows that the close lattice analogies may be related to a similar atomic arrangement. Apart from the differences in chemical formula (F:Cl ratio 1:1 in sulphohalite), the main difference in the structural framework consists of the unequal number of Na^+ sheets (six in sulphohalite) and in the SO_4^{2-} tetrahedra orientation.

THE multiple salts having compositions ranging from $\text{Na}_3\text{SO}_4\text{F}$ to $\text{Na}_6(\text{SO}_4)_2\text{FCl}$ form an interesting class of minerals closely related by chemical formula and structural analogies. Neglecting the end-members of the Na_2SO_4 -NaF-NaCl ternary system, the minerals presently known as distinct phases are:

kogarkoite,	$\text{Na}_3\text{SO}_4\text{F}$,	monoclinic;
schairerite,	$\text{Na}_{21}(\text{SO}_4)_7\text{F}_6\text{Cl}$,	trigonal;
galeite,	$\text{Na}_{15}(\text{SO}_4)_5\text{F}_4\text{Cl}$,	trigonal;
sulphohalite,	$\text{Na}_6(\text{SO}_4)_2\text{FCl}$,	cubic.

A description of these natural phases occurs in two recent papers (Brown and Pabst, 1971; Pabst and Sharp, 1973). The structures of the first three phases may be related to that of sulphohalite (Watanabe, 1934; Pabst, 1934; Sakamoto, 1968) on the basis of cell dimensions.

The present study is a first contribution to the clarification of the structural relationships in this family of minerals.

Schairerite was described by Foshag (1931) as a new mineral from Searles Lake evaporites, California. Its chemical analysis indicated that the composition was

$\text{Na}_2\text{SO}_4 \cdot \text{Na}(\text{F}_{0.814}\text{Cl}_{0.186})$. The first X-ray study was performed by Frondel (1940) on a single crystal and a hexagonal cell with a 12.12 Å, c 19.19 Å, $Z = 21$ was derived.

Wolfe and Caras (1951) determined the trigonal symmetry of the mineral and assigned a different unit-cell, with a volume $1/3$ of that proposed by Frondel, the same c axis and an a period of 7.05 Å. In 1963 Pabst *et al.* indicated that the diffraction symmetry of schairerite is $\bar{3}1mP$. The unit-cell has a 12.17 Å, c 19.29 Å, $Z = 21$ in agreement with Frondel's results, with a strongly marked pseudo-cell corresponding to the cell proposed by Wolfe and Caras. This pseudo-cell corresponds to the morphological setting of Foshag. The transformation matrix from the actual setting to that of the pseudo-cell is $[\frac{2}{3}, \frac{1}{3}, 0/\frac{1}{3}, \frac{1}{3}, 0/0, 0, 1]$ thus giving a diffraction symmetry of the pseudo-cell of $\bar{3}m1P$.

A microprobe study by Brown and Pabst (1971) showed that schairerite is remarkably constant in Cl and F content with a cell content equal to $\text{Na}_{63}(\text{SO}_4)_{21}\text{F}_{18}\text{Cl}_3$ and, on the basis of structural analogies with sulphohalite, that lattice parameters close to the experimental ones may be predicted for this cell content.

Experimental. For the structural study a sample from the type locality, Searles Lake, was employed. A 0.68 mm diameter sphere was mounted on a Philips PW 1100 automated diffractometer with Mo radiation and graphite monochromator. The cell dimensions, determined from a least-squares analysis of 2θ values for 25 reflections, are a 12.197 ± 0.004 Å and c 19.259 ± 0.011 Å. The calculated density, 2.619 g cm^{-3} , is in close agreement with the observed value of 2.616 g cm^{-3} (Brown and Pabst, 1971). The lack of systematic extinctions is compatible with space groups $P\bar{3}1m$, $P31m$, and $P312$.

Intensity data were collected by the $\omega/2\theta$ scan technique over the range $6^\circ \leq 2\theta \leq 60^\circ$. A total of 2921 reflections were collected of which 385 had intensity less than $3\sigma(I)$ and were considered unobserved and excluded from further calculations.¹ The data were corrected for Lorentz and polarization factors, while absorption corrections were neglected because of the low μR value (0.33).

Structure analysis. It was realized that, in the solution of the atomic arrangement of schairerite, a first important step could be represented by determining the average structure of the pseudo-cell, which must be near to the true one. In this attempt the results of logical symbolic addition and a 3-D Patterson function computed from diffraction effects of the pseudo-cell were taken into consideration together with structural information derived from the structure of sulphohalite on the basis of close analogies in the series and assuming, initially, that schairerite belongs to the centrosymmetric space group. These methods allowed the positioning of the 24 heaviest atoms (sulphur and chlorine), 54 out of a total of 63 Na atoms, 72 out of a total of 84 oxygen atoms, and 15 out of a total of 18 F atoms in the cell. After several cycles of isotropic least-squares refinement (traditional R index = 0.34), it was realized that a satisfactory structural arrangement is incompatible with the assumption of the centrosymmetric $P\bar{3}1m$ space group ($P\bar{3}m1$ considering the pseudo-cell only).

¹ $\sigma(I) = [P + 0.25(B_1 + B_2)(T_P/T_B)^2 + (0.03 I)^2]^{1/2}$ where P is the total peak count in a scan of time T_P , B_1 and B_2 are the background counts each in a time T_B , I is the intensity equal to $[P - 0.5(T_P/T_B)(B_1 + B_2)]$.

Consequently, a rearrangement of atoms in the space group $P3_1m$ was made, and the atomic framework could be completed by means of successive Fourier syntheses.

When the last atomic positions were introduced into the calculation the R value fell to 0.22. Fluorine and chlorine positions were still undistinguished and the scattering factor employed was that of fluorine. The over-all B value was 1.5 \AA^2 . When isotropic thermal parameters were refined and the three chlorine atoms distinguished from the fluorines, the R value decreased to 0.15 indicating that the average structure must be very close to the true one. The relation between the sub-cell and the true cell was studied to investigate how far the true structure deviates from the average structure.

A Patterson synthesis was then computed employing only F^2 s of reflections not belonging to the pseudo-cell. This partial Patterson function was investigated for deriving the 'distortion structure' (Takeuchi, 1972) originating from the substructure.

This function showed heaviest maxima and minima on the three-fold axes, suggesting that the rearrangement in the true cell mainly involves the z co-ordinates of sulphur and chlorine atoms located on these axes. This may be explained by noting that in the space group $P3_1m$ two sets of three-fold axes are present, whilst in the sub-cell these axes are equivalent by translation. In this way a first displacement of z co-ordinates for atoms on the three-fold axes was evaluated and better agreement between observed and calculated data was obtained. In addition, the partial Patterson function showed additional peaks around three-fold axes, at sulphur-oxygen distances, which could be interpreted as originating from different orientations of SO_4^{2-} groups. This was confirmed by a difference Fourier map, which revealed the different orientation of SO_4^{2-} tetrahedra located at $0, 0, z$ compared with those located at $\frac{2}{3}, \frac{1}{3}, z$ and $\frac{1}{3}, \frac{2}{3}, z$. Four cycles of isotropic refinement by full-matrix least-squares methods applied to all observed reflections led to a complete structural framework with an R value of 0.070.

Atomic scattering factors for S, Cl^- , F^- , Na^+ , and O^- were taken from the *International Tables for X-ray Crystallography* (1962). Six structure factors were excluded from the last refinement because they were suspected to be affected by extinction. Atomic co-ordinates and isotropic temperature factors are listed in Table I. A table containing observed and calculated structure factors is deposited in the library of the Department of Mineralogy, British Museum (Natural History), whence copies may be purchased.

Discussion. A schematic view of the structure of schairerite, projected along the c axis, is shown in fig. 1*a*. In the figure an overlap of halogen, sulphur, and some of the oxygen atoms occurs on three-fold axes and pseudo-axes (marked by \blacktriangle and \triangle symbols, respectively). Sulphur tetrahedra and Na^+ positions are shown together with the outline of the sub-cell. S-O bond lengths and bond angles with their standard deviations are included in Tables II and III, and other atomic distances are included in a table deposited along with the table of structure factors.

All tetrahedra of SO_4^{2-} anions are oriented with one of their three-fold axes parallel to the c direction. The tetrahedra with sulphur atoms located at $00z$, $\frac{1}{3} 0 z$, $0 \frac{1}{3} z$ and $\frac{2}{3} \frac{2}{3} z$ in the unit cell have the S-O bond along the c direction coincident with the negative sense of the translation while those at $\frac{1}{3} \frac{2}{3} z$, $\frac{2}{3} \frac{1}{3} z$, $\frac{2}{3} 0 z$, $0 \frac{2}{3} z$, and $\frac{1}{3} \frac{1}{3} z$ have the above-mentioned bond coincident with the positive sense of the c axis. The

TABLE I. Fractional atomic co-ordinates and isotropic thermal parameters with standard deviations in parentheses

Atom	x/a	y/b	z/c	$B(\text{\AA}^2)$	Atom	x/a	y/b	z/c	$B(\text{\AA}^2)$
Cl	0	0	0	0.73 (6)	F (3)	0.3486 (5)	0	0.5674 (5)	0.98 (11)
Cl'	2/3	1/3	0.0296 (2)	1.87 (7)	F (4)	0.6620 (7)	0	0.3131 (6)	1.45 (11)
S (1)	0	0	0.2376 (4)	1.05 (9)	F (5)	0.6753 (6)	0	0.1666 (5)	1.14 (11)
S (1')	2/3	1/3	0.2532 (4)	1.00 (6)	F (6)	0.3262 (6)	0	0.7175 (5)	0.74 (10)
S (2)	0	0	0.7782 (5)	0.95 (9)	O (1A)	0	0	0.1631 (12)	3.05 (39)
S (2')	2/3	1/3	0.7950 (4)	0.75 (6)	O (1B)	0.8884 (7)	0	0.2636 (5)	1.17 (14)
S (3)	0	0	0.5074 (4)	0.90 (10)	O (1A')	2/3	1/3	0.3301 (8)	1.89 (23)
S (3')	2/3	1/3	0.5266 (4)	0.72 (5)	O (1B')	0.6683 (5)	0.2201 (7)	0.2318 (5)	1.98 (13)
S (4)	0.6699 (3)	0	0.6659 (4)	0.81 (4)	O (2A)	0	0	0.7026 (10)	1.79 (29)
S (5)	0.6672 (3)	0	0.9387 (4)	0.90 (4)	O (2B)	0.1140 (7)	0	0.8064 (6)	1.22 (14)
S (6)	0.3366 (3)	0	0.3673 (4)	0.83 (4)	O (2A')	2/3	1/3	0.8717 (6)	0.75 (14)
S (7)	0.3344 (3)	0	0.0933 (4)	0.62 (4)	O (2B')	0.5502 (7)	0.2158 (7)	0.7701 (5)	1.91 (12)
Na (1)	0.5152 (4)	0	0.5166 (4)	1.49 (9)	O (3A)	0	0	0.4317 (9)	1.15 (25)
Na (1')	0.1591 (4)	0.3340 (5)	0.5147 (4)	1.25 (6)	O (3B)	0.1130 (7)	0	0.5320 (5)	1.13 (13)
Na (2)	0.8128 (4)	0	0.3780 (4)	1.05 (8)	O (3A')	2/3	1/3	0.6043 (7)	1.16 (17)
Na (2')	0.4788 (3)	0.3318 (4)	0.3846 (4)	1.31 (6)	O (3B')	0.6720 (5)	0.2209 (6)	0.5021 (5)	1.76 (12)
Na (3)	0.1892 (4)	0	0.9294 (5)	1.23 (9)	O (4A)	0.6771 (8)	0	0.7416 (6)	1.13 (15)
Na (3')	0.8470 (3)	0.3359 (4)	0.9339 (4)	1.22 (6)	O (4B)	0.5517 (7)	0	0.6460 (6)	1.13 (14)
Na (4)	0.1759 (4)	0	0.6486 (4)	1.20 (9)	O (4C)	0.7834 (6)	0.1167 (6)	0.6403 (5)	1.36 (10)
Na (4')	0.8448 (3)	0.3337 (4)	0.6527 (4)	1.25 (6)	O (5A)	0.6678 (8)	0	0.0146 (6)	0.98 (13)
Na (5)	0.8236 (5)	0	0.0957 (5)	1.84 (11)	O (5B)	0.5527 (7)	0	0.9142 (7)	1.26 (17)
Na (5')	0.4783 (4)	0.3312 (4)	0.1034 (4)	1.77 (7)	O (5C)	0.7808 (6)	0.1154 (6)	0.9133 (5)	1.14 (10)
Na (6)	0.4879 (5)	0	0.7928 (5)	1.22 (10)	O (6A)	0.3384 (8)	0	0.2897 (6)	1.32 (14)
Na (6')	0.1515 (3)	0.3345 (4)	0.7941 (4)	0.98 (6)	O (6B)	0.4475 (7)	0	0.3971 (6)	1.52 (17)
Na (7)	0.5180 (5)	0	0.2357 (5)	1.50 (11)	O (6C)	0.3356 (8)	0.1125 (6)	0.3934 (5)	1.51 (11)
Na (7')	0.1811 (4)	0.3334 (5)	0.2391 (4)	1.58 (7)	O (7A)	0.3358 (9)	0	0.0167 (6)	1.66 (16)
F (1)	0.6858 (5)	0	0.4658 (5)	1.37 (12)	O (7B)	0.4461 (8)	0	0.1203 (7)	1.85 (20)
F (2)	0.3396 (6)	0	0.8636 (5)	0.86 (10)	O (7C)	0.3342 (9)	0.1123 (7)	0.1204 (5)	1.83 (12)

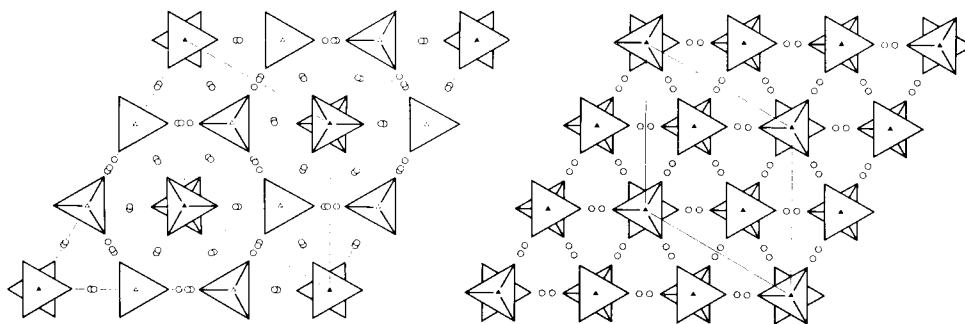


FIG. 1a (left). SO_4^{2-} tetrahedra and Na^+ positions in schairerite viewed along c direction. 1 chlorine, 3 sulphur, and 3 oxygen atoms lie on ternary axes (\blacktriangle), 3 fluorine, 2 sulphur, and 2 oxygen atoms lie on pseudo-ternary axes (Δ). The outline of the pseudo-cell is drawn by broken lines. b (right). SO_4^{2-} tetrahedra and Na^+ positions in sulphohalite viewed along the direction of one set of ternary axes. 1 chlorine, 1 fluorine, 2 sulphur, and 2 oxygen atoms lie on ternary axes (\blacktriangle). The trigonal cell corresponding to the sub-cell of schairerite is drawn by full lines.

TABLE II. Sulphur–oxygen distances. Standard deviations are $\leq 0.010 \text{ \AA}$

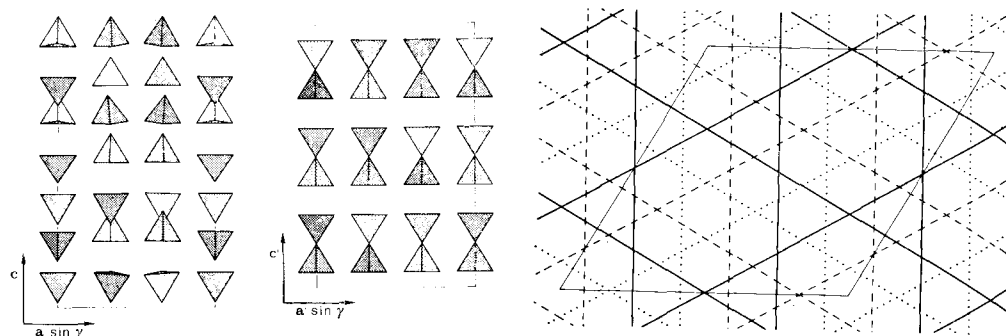
S (1) – O (1A)	1.434 Å	S (4) – O (4A)	1.462 Å
– O (1B) × 3	1.451	– O (4B)	1.492
S (1') – O (1A')	1.482	– O (4C) × 2	1.488
– O (1B') × 3	1.451	S (5) – O (5A)	1.462
S (2) – O (2A)	1.458	– O (5B)	1.474
– O (2B) × 3	1.493	– O (5C) × 2	1.480
S (2') – O (2A')	1.476	S (6) – O (6A)	1.496
– O (2B') × 3	1.506	– O (6B)	1.470
S (3) – O (3A)	1.458	– O (6C) × 2	1.468
– O (3B) × 3	1.457	S (7) – O (7A)	1.476
S (3') – O (3A')	1.496	– O (7B)	1.459
– O (3B') × 3	1.482	– O (7C) × 2	1.467

TABLE III. O–S–O angles. Standard deviations are $\leq 0.5^\circ$

O (1A) – S (1) – O (1B) × 3	110.2°	O (4B) – S (4) – O (4C) × 2	110.6°
O (1B) – S (1) – O (1B) × 3	108.7	O (4C) – S (4) – O (4C)	111.9
O (1A') – S (1') – O (1B') × 3	106.5	O (5A) – S (5) – O (5B)	108.9
O (1B') – S (1') – O (1B') × 3	112.3	O (5A) – S (5) – O (5C) × 2	109.1
O (2A) – S (2) – O (2B) × 3	111.3	O (5B) – S (5) – O (5C) × 2	109.4
O (2B) – S (2) – O (2B) × 3	107.6	O (5C) – S (5) – O (5C)	110.9
O (2A') – S (2') – O (2B') × 3	108.6	O (6A) – S (6) – O (6B)	112.1
O (2B') – S (2') – O (2B') × 3	110.4	O (6A) – S (6) – O (6C) × 2	110.4
O (3A) – S (3) – O (3B) × 3	109.0	O (6B) – S (6) – O (6C) × 2	107.7
O (3B) – S (3) – O (3B) × 3	110.0	O (6C) – S (6) – O (6C)	108.2
O (3A') – S (3') – O (3B') × 3	108.5	O (7A) – S (7) – O (7B)	110.2
O (3B') – S (3') – O (3B') × 3	110.4	O (7A) – S (7) – O (7C) × 2	111.1
O (4A) – S (4) – O (4B)	108.3	O (7B) – S (7) – O (7C)	108.1
O (4A) – S (4) – O (4C) × 2	107.6	O (7C) – S (7) – O (7C)	108.0

orientation of SO_4^{2-} tetrahedra is shown in fig. 2*a*. Bond lengths and angles in SO_4^{2-} tetrahedra are regular and the average S–O bond distance calculated from 40 independent values is 1.473 Å, in a range 1.434–1.506 Å.

Na^+ ions are located on seven sheets perpendicular to the *c* axis. The Na^+ ions in each sheet are arranged in an array built up of hexagons and triangles, each hexagon being surrounded by six triangles and each triangle by three hexagons. The sheets are



FIGS. 2 and 3: FIG. 2*a* (left). SO_4^{2-} tetrahedra in schairerite viewed along the *a* direction. *b* (right). SO_4^{2-} tetrahedra in sulphohalite viewed along the direction corresponding to *a* in schairerite. FIG. 3. The schematic arrangement of Na^+ ions at the corners of hexagons and triangles: full lines for Na^+ ions at $z \approx 0.24, 0.52, \text{ and } 0.79$ (planes A); broken lines for Na^+ ions at $z \approx 0.10$ and 0.38 (planes B); dotted lines for Na^+ ions at $z \approx 0.65$ and 0.93 (planes C).

shifted with respect to each other in such a way that the centres of the triangles and hexagons are always located on ternary axes and pseudo-axes. Taking into account the shifts of the sheets, they can be divided in three sets and their succession is BABACAC. The arrangement of sodium ions is roughly centrosymmetric as shown in the schematic view of the sheets of Na^+ ions drawn in fig. 3. Chlorine, fluorine, and sulphur ions on the three-fold axes and pseudo-axes are accommodated at particular positions with reference to the Na^+ sheets: sulphur atoms lie on the sheets at the centre of each hexagon, whilst halogen atoms lie between the sheets midway between the centres of two triangles. The larger size of Cl ions causes a loose sandwiching of the Na^+ atom sheets, separated approximately by 3.23 Å, while the other sheets sandwiching fluorine atoms are separated by values in the range 2.59–2.77 Å (average value 2.67 Å).

All fourteen asymmetric Na^+ ions exhibit the co-ordination $\text{Na}(\text{OSO}_3)_4\text{X}_2$ with $\text{X}_2 = \text{F}_2$ or FCl in distorted octahedra. In six cases (Na (1), Na (1'), Na (3), Na (3'), Na (5), and Na (5')) a *trans* configuration of halogen ligands is observed whilst the others show a *cis* configuration. The *trans* configuration is always present in the four $\text{Na}(\text{OSO}_3)_4\text{FCl}$ octahedra. Interatomic distances are in agreement with those reported in literature: Na–Cl bonds range from 2.68 to 2.86 Å, Na–F bonds from 2.20 to 2.62 Å, Na–O bonds from 2.36 to 2.63 Å. The average values are: Na–Cl 2.77 Å (4 values), Na–F 2.31 Å (24 values), Na–O 2.43 Å (56 values).

If we consider the connections among the Na^+ co-ordination octahedra in the seven sheets, five motifs can be distinguished and are sketched in figs. 4a, 4b, 4c, 4d, and 4e. The first motif belongs to the two sheets corresponding to sodium ions approximately at $z = 0.24$ and $z = 0.79$. The two sheets are related by symmetry pseudo-centres. In these two sheets three octahedra are grouped to form a triplet in which each octahedron shares two faces with the other two octahedra, all together sharing an edge parallel to c direction. Each triplet is connected with six surrounding triplets through three corners (fig. 4a). A similar motif occurs for octahedral sheets surrounding Na^+ ions at $z \approx 0.38$ and $z \approx 0.65$. In fact the grouping of triplets is analogous to that previously described, the difference consisting in lack of ternary symmetry in single triplets. The sheet with Na^+ ions at $z \approx 0.38$ is shown in fig. 4b. The difference from the other sheet (Na^+ at $z \approx 0.65$) arises in the orientation and location of the motif in the unit cell but not in the shape. When we consider the two adjacent octahedral sheets corresponding to Na^+ ions at $z \approx 0.93$ and $z \approx 0.10$ and including chlorine atoms, it can be seen that both of them consist of triplets of similar shape to those previously described. In the first case, each of these triplets is connected with similar triplets twice by common edges and once by a common corner (fig. 4c). In the second case the connection occurs in the opposite way, once by a common edge and twice by common corners (fig. 4d). The sheet of octahedra surrounding Na^+ ions at $z \approx 0.52$ is built up of groups of nine polyhedra sharing edges 'two by two'; in each of these groups three corners are shared by three different octahedra. Each group is connected to six equivalent groups by six corners (fig. 4e).

Each of the seven sheets is linked to the adjacent ones through faces or edges of co-ordination octahedra or both, with the exception of the two sheets including chlorine atoms, which share only corners represented by these atoms. Therefore the crystal structure of schairerite may be described as consisting of a three-dimensional framework of Na^+ co-ordination octahedra in a very tight packing.

Co-ordination around halogen atoms is always sixfold with Na^+ atoms at the corners of distorted octahedra. Each oxygen atom is linked by a sulphur atom and by three Na^+ cations. Therefore the charge balance for halogen and oxygen atoms is quite perfect.

The nature of the pseudo-symmetry giving rise to the sub-cell with $a = 7.042 \text{ \AA}$ can be easily understood from fig. 1a. It can be noted that the orientation of SO_4^{2-} groups is not the same along the two non-equivalent sets of ternary axes, causing a lowering of symmetry in the motif. Also slight differences in the z co-ordinates of chlorine and sulphur atoms on these axes, which cannot be revealed in the projection, affect motif symmetry but in a less significant way. The arrangement of the remaining atoms is very close to the symmetry of the sub-cell; for example, if we look at the octahedral sheets around Na^+ ions, it can be argued from fig. 4a that two of the seven sheets are consistent with the sub-cell previously described. We may conclude that the different orientation of sulphate groups along the three-fold axes is the main reason justifying a description of the crystal structure of schairerite in the larger cell.

Relationships between schairerite and sulphohalite. There are evident similarities between schairerite and sulphohalite. The chemical formula of sulphohalite, $\text{Na}_6(\text{SO}_4)_2\text{FCl}$, has the same $\text{Na}:\text{SO}_4:X$ (with $X = \text{F} + \text{Cl}$) ratio as in schairerite.

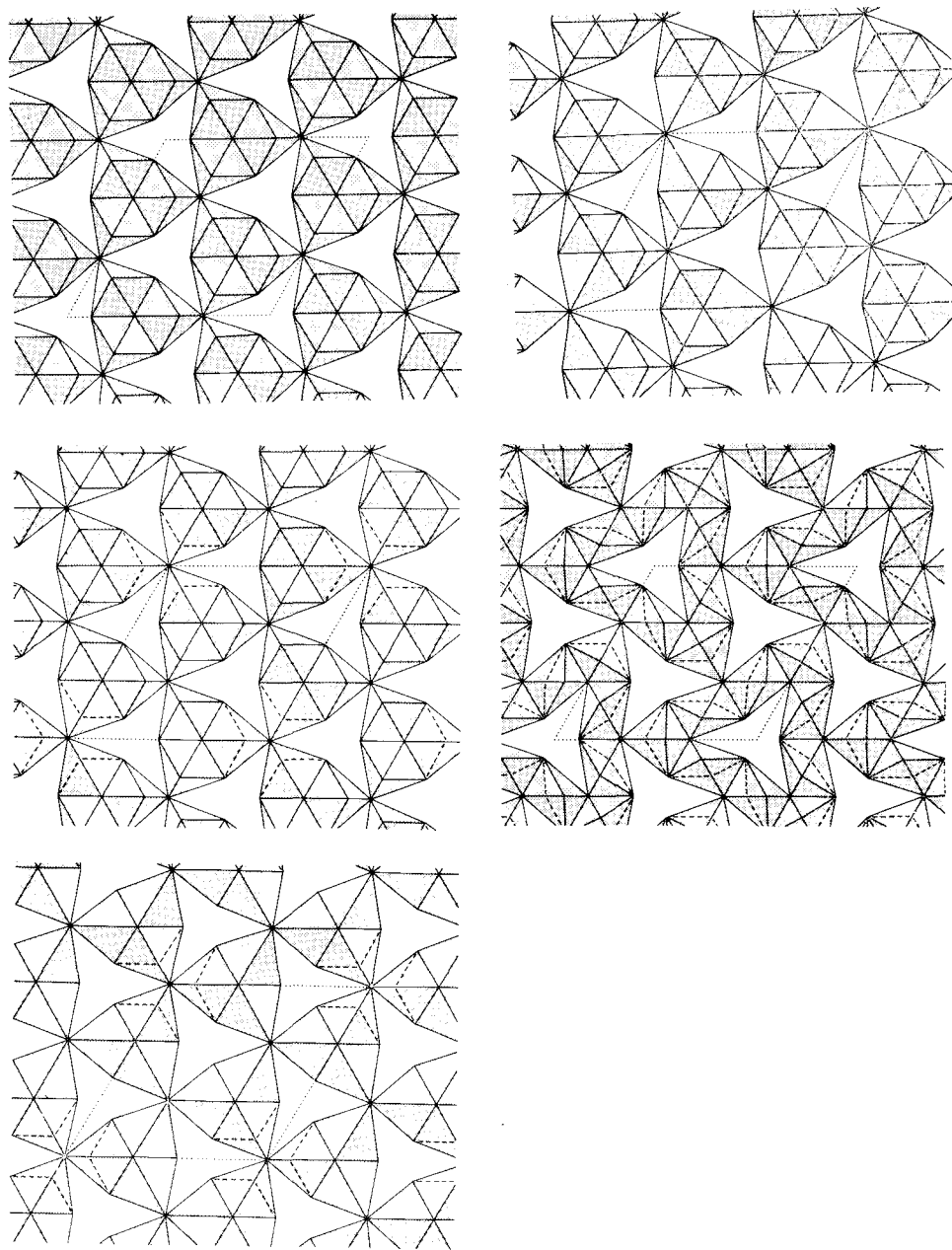


FIG. 4a (top left). The structural motif of co-ordination-distorted octahedra around Na^+ ions at $z \approx 0.79$ (similar motif for $z \approx 0.24$). b (middle left). The structural motif of co-ordination-distorted octahedra around Na^+ ions at $z \approx 0.38$ (similar motif for $z \approx 0.65$). c (bottom left). The structural motif of co-ordination-distorted octahedra around Na^+ ions at $z \approx 0.93$. d (top right). The structural motif of co-ordination-distorted octahedra around Na^+ ions at $z \approx 0.10$. e (bottom right). The structural motif of co-ordination-distorted octahedra around Na^+ ions at $z \approx 0.52$.

The chemical difference consists only in the F:Cl ratio, which is 1:1 in sulphohalite and 6:1 in schairerite. The similarities in chemical formula and genetic conditions (the two minerals are present among the lower salts of the Searles Lake evaporite basin) allows reasonable structural analogies between sulphohalite and schairerite to be drawn. Indeed, the cubic face-centred unit cell of sulphohalite may be described as a hexagonal setting in a trigonal cell corresponding to the sub-cell of schairerite but with a shorter c axis (Brown and Pabst, 1971). The lattice translations give rise to a 7.119 Å, c 17.438 Å for sulphohalite and a 7.042 Å, c 19.259 Å for schairerite. The symmetry of the hexagonal cell of sulphohalite is $P\bar{3}m1$, whilst that of the sub-cell of schairerite, lacking an inversion centre, is $P3m1$. The cell contents are $\text{Na}_{18}(\text{SO}_4)_6\text{F}_3\text{Cl}_3$ and $\text{Na}_{21}(\text{SO}_4)_7\text{F}_6\text{Cl}$ respectively. The similarities in structural arrangement become evident when the ab projection of schairerite (fig. 1a) is compared with the same projection of sulphohalite (fig. 1b). In this figure the unit cell of sulphohalite is built up on the corresponding lattice translations of the true cell of schairerite. The lattice translations corresponding to the sub-cell of schairerite are shown by full lines.

In the trigonal cell of sulphohalite, six atoms (1 Cl, 1 F, 2 S, and 2 O) are superimposed along the three-fold axes in a centrosymmetric arrangement. The orientation of tetrahedra along every axis is, in turn, 'up-down' (fig. 2b) and this feature can be considered as the prominent difference from schairerite in the structural framework. The lattice of sodium ions shows close analogies with schairerite and consists of six sheets formed by nearly regular hexagons and triangles, as in schairerite. Using the same notation the succession of sheets is BACBAC with a separation of two consecutive sheets of 2.91 Å. Apart from orientation and location in the unit cell, the sheets of octahedra around Na^+ ions viewed along a set of ternary axes are identical and the motif of each sheet corresponds to that described for two of the seven sheets of schairerite (fig. 4a).

Analogies in chemical formula and in lattice dimensions support the existence of close structural relationships also with galeite and kogarkoite. These structural relationships will be better considered when crystallographic studies on these minerals, presently in progress, are completed.

Acknowledgements. We are grateful to Professor C. M. Gramaccioli who supplied us with one of the samples employed in the present investigation. This work was supported by the Italian Consiglio Nazionale delle Ricerche.

REFERENCES

- BROWN (F. H.) and PABST (A.), 1971. *Amer. Min.* **56**, 174.
FOSHAG (W. F.), 1931. *Ibid.*, **16**, 133.
FRONDEL (C.), 1940. *Ibid.*, **25**, 338.
International Tables for X-ray Crystallography, 1962, **3**, 202.
PABST (A.), 1934. *Zeits. Krist.* **89**, 514.
— SAWYER (D. L.), and SWITZER (G.), 1963. *Amer. Min.* **48**, 485.
— and SHARP (W. N.), 1973. *Ibid.*, **58**, 116.
SAKAMOTO (Y.), 1968. *J. Sci. Hiroshima Univ.*, Ser. A-II **32**, 101.
TAKEUCHI (Y.), 1972. *Zeits. Krist.* **135**, 120.
WATANABE (T.), 1934. *Proc. Imperial Acad. (Japan)*, **10**, 575.
WOLFF (C. W.) and CARAS (A.), 1951. *Amer. Min.* **36**, 912.

[Manuscript received 5 March 1974]